IEEE Access
Multidisciplinary | Rapid Review | Open Access Journal

Received January 14, 2020, accepted March 28, 2020, date of publication April 3, 2020, date of current version April 21, 2020.

Digital Object Identifier 10.1109/ACCESS.2020.2985569

Branch Line Couplers With Small Size and Harmonic Suppression Based on Non-Periodic Step Impedance Shunt Stub (SISS) Loaded Lines

JAN COROMINA, (Student Member, IEEE), PARIS VÉLEZ, (Member, IEEE), JORDI BONACHE, (Member, IEEE), AND FERRAN MARTíN, (Fellow, IEEE)
CIMITEC, Departament d'Enginyeria Electrònica, Universitat Autònoma de Barcelona, 08193 Bellaterra, Spain

Corresponding author: Jan Coromina (jan.coromina@uab.cat)

This work was supported in part by the MINECO-Spain under Project TEC2016-75650-R, in part by the Generalitat de Catalunya under Project 2017SGR-1159, in part by the Institució Catalana de Recerca i Estudis Avançats (who awarded Ferran Martín), and in part by the FEDER Funds. The work of Paris Vélez was supported by the Ministerio de Ciencia, Innovación y Universidades through the Juan de la Cierva Fellowship under Grant IJCI-2017-31339.

ABSTRACT This paper presents branch line couplers with compact size and harmonic suppression based on non-periodic reactively loaded artificial lines. The reactive loading elements of the lines are step impedance shunt stubs (SISSs). Such elements provide transmission zeros, which are useful to efficiently suppressing the harmonic content of the device. Moreover, by virtue of reactive loading, the reported artificial lines exhibit a slow wave effect of interest for device miniaturization. The combination of size, harmonic suppression efficiency, and design simplicity (with a clear design methodology) is of interest within the framework of artificial transmission lines and their application to the optimization of microwave passive components.

INDEX TERMS Branch line couplers, harmonic suppression, slow waves, step impedance shunt stub (SISS).

I. INTRODUCTION

Slow wave transmission lines are artificial lines, typically consisting of a host line loaded with reactive elements (either quasi-lumped or distributed), exhibiting a small phase velocity, as compared to the one of ordinary lines [1], [2]. By virtue of this small phase velocity, the guided wavelength in these lines is also small. Consequently, these artificial lines are useful for the implementation of distributed microwave components with compact size, where such (shorter) lines replace the ordinary (longer) lines. Most slow wave transmission lines are implemented by periodic reactive loading [3]–[37], and it has been argued that periodicity generates stop bands, useful for harmonic suppression, or for the implementation of devices with filtering capability. However, periodicity is not actually a requirement in order to implement harmonic-suppressed microwave devices.

In this paper, it is demonstrated that step impedance shunt stubs (SISSs) [38] are very interesting loading elements for slow wave transmission lines, as far as the resulting artificial lines combine small size, good harmonic suppression efficiency and simple design methodology [39]–[41]. The efficient harmonic suppression is achieved in this paper by truncating periodicity. Specifically, the SISSs are designed in order to exhibit identical susceptance at the design frequency (where the electrical length of the lines is given by circuit requirements), but different transmission zeros. By properly distributing the transmission zeros, a broad and controllable stop band can be generated, thereby suppressing the harmonic bands of the intended device very efficiently.

In this paper, such non-periodic artificial lines are applied to the implementation of compact and harmonic suppressed branch lines couplers. Many efforts have been recently devoted to the miniaturization and/or harmonic suppression in branch lines couplers [3], [6], [8], [11], [15], [23], [28]–[37], [42]–[56]. However, most of the reported implementations are based on periodic structures. It is shown in this paper that by loading the constitutive host lines of the branch line coupler with SISSs resonating at different frequencies, a set of transmission zeros can be generated. This represents a further degree of freedom in the design, and it is possible to achieve an efficient harmonic suppression. Particularly, very efficient rejection of the first harmonic band of the coupler, with a sharp roll-off in the response, is achieved by placing

The associate editor coordinating the review of this manuscript and approving it for publication was Flavia Grassi.

the first transmission zero at the position of the first harmonic (i.e., at $3f_0$, where f_0 is the operating frequency of the branch line coupler).

II. DESIGN OF THE NON-PERIODIC SISS-LOADED LINES

The main electrical parameters of the constitutive transmission lines, either ordinary or artificial, of a certain distributed microwave component are the characteristic impedance and the electrical length at the design frequency. Whereas in ordinary lines the characteristic impedance is not frequency dependent, in reactively loaded lines dispersion is unavoidable. Therefore, the equivalent to the characteristic impedance (i.e., the Bloch impedance in periodic lines, or, more generally, the image impedance in arbitrary networks), is no longer constant with frequency. Consequently, the characteristic impedance of the artificial lines under consideration, i.e., SISS-loaded lines, must be forced to satisfy the design requirement at the operating frequency of the designed device.

Let us designate as Z_B and θ the required characteristic impedance and electrical length, respectively, of the artificial line at the operating frequency, f_0. Let us also assume that the line is composed of N cells with identical electrical length, βl (so that $\theta = N \cdot \beta l$). The parameters of the constitutive cells of the SISS-loaded lines (Fig. 1) are given by the following set of equations [2]:

$$\cos(\beta l) = \cos(kl) - \frac{B_p Z_0}{2}\sin(kl) \tag{1}$$

$$Z_B = \frac{Z_0}{\sin(\beta l)}\left(\sin(kl) - B_p Z_0 \sin^2(kl/2)\right) \tag{2}$$

$$swr = \frac{v_{pL}}{v_{po}} = \frac{\omega/\beta}{\omega/k} = \frac{kl}{\beta l} \tag{3}$$

where kl and Z_0 are the electrical length and characteristic impedance, respectively, of the host line, and B_p is the susceptance of the SISS resonator. In expression (3), *swr* is the slow-wave ratio, a relevant parameter that determines the level of compactness of the lines (the *swr* is a design specification for artificial lines).

Note that the three previous equations determine univocally the three electrical parameters of the cell, kl, Z_0 and B_p. However, since B_p is the susceptance of the SISS, and such elements are described by a series resonator, with inductance L_i and capacitance C_i, respectively, it follows that such reactive elements (L_i and C_i) are not univocally determined from the previous equations. Indeed, line periodicity is truncated by choosing different combinations of L_i and C_i, in order to generate different transmission zeros, as previously mentioned. From the value of B_p, determined from the solution of equations (1)-(3), and given by [38]:

$$B_p = \frac{C_i\omega_0}{1 - L_i C_i \omega_0^2} \tag{4}$$

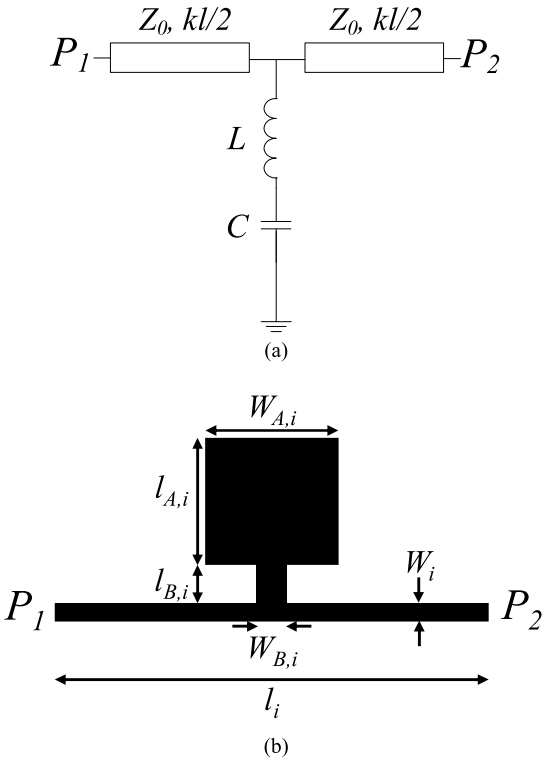

FIGURE 1. Equivalent circuit model of the SISS-loaded unit cell of the considered slow wave artificial line (a) and typical topology (b). Relevant dimensions are indicated. The subindex *i* refers to the specific cell.

and the position of the transmission zero associated to a certain SISS, i.e.,

$$f_{z,i} = \frac{1}{2\pi\sqrt{L_i C_i}} \tag{5}$$

the elements L_i and C_i are perfectly determined. In (4), $\omega_0 = 2\pi f_0$ is the angular operating frequency.

III. BRANCH LINE COUPLER DESIGN AND RESULTS

Branch line couplers are implemented by means of two pairs of $\theta = 90°$ lines. The characteristic impedance of one of the pairs is $Z_B = 50\ \Omega$, whereas the other line pair exhibits a characteristic impedance of $Z_B = 35.35\ \Omega$. Let us consider that the operating frequency is $f_0 = 1$ GHz and that the number of cells of each line is $N = 2$. With $N = 2$, the onset of the stop band is comprised between f_0 and $3f_0$, so that the first harmonic band is suppressed and, at the same time, the response in the region of interest is kept unaltered, as it was demonstrated in [23] (where the electrical length of the cells is identical, i.e., 45°).

Since the coupler involves four slow wave transmission lines, and consequently eight SISSs (one SISS per cell), several transmission zeros can be generated with the SISS of the particular lines. In the present paper, we have considered as a first step two different transmission zeros, one of them located at $3f_0$ (for the efficient suppression of the first harmonic band, located at that frequency), and the other one positioned at $7f_0$. With such transmission zero at $7f_0$, we do not only achieve

TABLE 1. Electrical parameters for each cell.

	Cell 1	Cell 2	Cell 3	Cell 4
Z_B (Ω)	50	50	35.35	35.35
βl (degrees)	45	45	45	45
swr	0.6	0.6	0.5	0.5
f_z / f_0	3	7	3	7
kl (degrees)	27	27	22.5	22.5
Z_0 (Ω)	86.27	86.27	73.61	73.61
L (nH)	2.118	0.353	1.293	0.215
C (pF)	1.329	1.464	2.177	2.399

a substantial rejection level of the harmonic located at that frequency, but also a very wide stop band, as it will be shown later.

Both the 50-Ω and 35.35-Ω lines have been designed with one cell exhibiting the transmission zero at $3f_0$ and the other one with the transmission zero located at $7f_0$. The electrical length of all the cells is 45°. Concerning the slow wave ratio, it has been set to $swr = 0.5$ for the 35.35-Ω cells and to $swr = 0.6$ for the 50-Ω cells. The reason is that with the considered substrate for circuit fabrication, the *Rogers 4003C* with dielectric constant $\varepsilon_r = 3.55$, thickness $h = 0.2032$ mm and loss tangent $\tan\delta = 0.0022$, line parameters provide extreme geometrical values (width of the host line) for the 50-Ω line with $swr = 0.5$.

The electrical parameters for the four considered cells, and the values of kl, Z_0, L and C that result by solving equations (1)-(5) are given in Table 1. Figure 2 depicts the frequency dependence of the electrical length and characteristic impedance of the designed 35.35-Ω and 50-Ω slow-wave artificial lines, as well as the frequency response, inferred from the circuit simulation of the schematic using *Keysight ADS*. For the 35.35-Ω/50-Ω line, the reference impedance of the ports has been considered to be 35.35 Ω/50 Ω in order to easily verify that the required value of the characteristic impedance ($Z_B = 35.35$ Ω/50 Ω) at f_0 is satisfied (it is indicated by the reflection zero at that frequency). It can be seen from Fig. 2 that the required electrical length at f_0 ($\theta = 90°$) is satisfied in both lines. Finally, the frequency responses, with transmission zeros located at 3 GHz and 7 GHz, exhibit a wide stop band with significant rejection level.

In the next step, we have inferred the response of the coupler at the schematic level (also using the circuit solver of *Keysigth ADS*) by assembling the designed lines. The schematic and the coupler responses are depicted in Figs. 3 and 4, respectively. It can be seen that the coupler response in the region of interest is very similar to the one of the conventional coupler (the response is also included in Fig. 4). However, the coupler based on the artificial

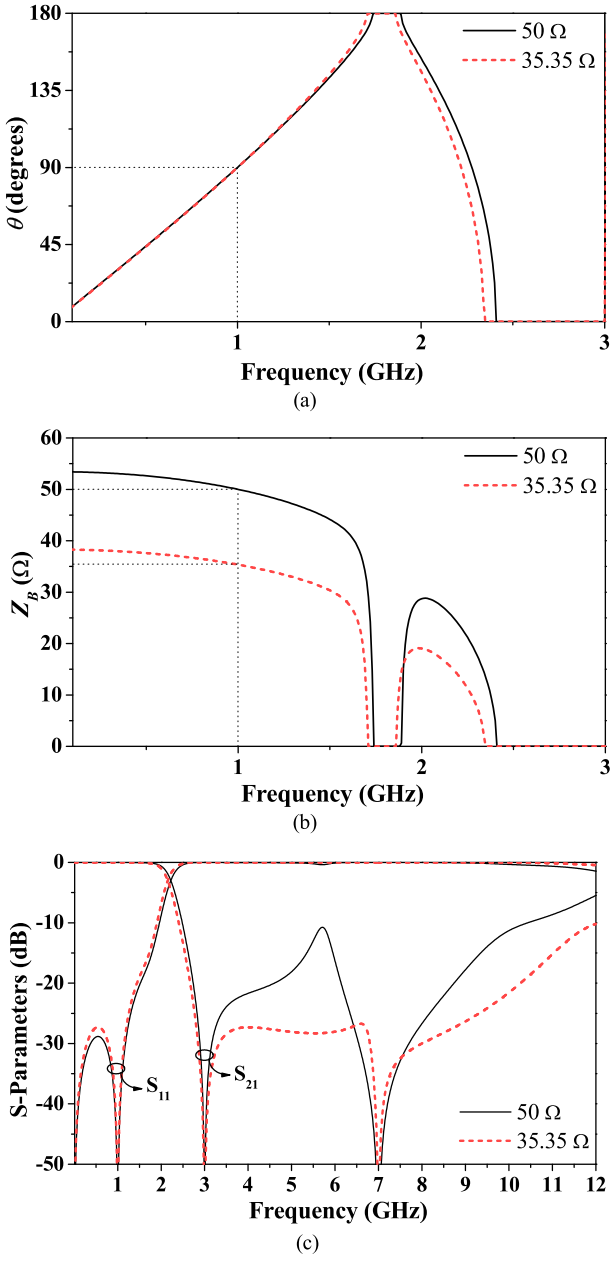

FIGURE 2. Electrical length (a) characteristic impedance (b) and frequency response (c) of the designed 90° slow-wave 35.35-Ω and 50-Ω artificial lines, inferred from circuit simulation.

lines exhibits good harmonic suppression, by virtue of the presence of reactive elements (providing transmission zero frequencies).

Subsequently, the layout of the proposed coupler has been synthesized. For that purpose, the transmission line calculator included in *Keysight ADS* has been used. The width and length of the host lines for the 35.35-Ω and 50-Ω unit cells has been found to be the one indicated in Table 2, where the geometry of the cells is provided, in reference to Fig. 1 (b). As for the dimensions of the SISS, we have set the width of the inductive line to 0.2 mm, close to the minimum strip width achievable with the available fabrica-

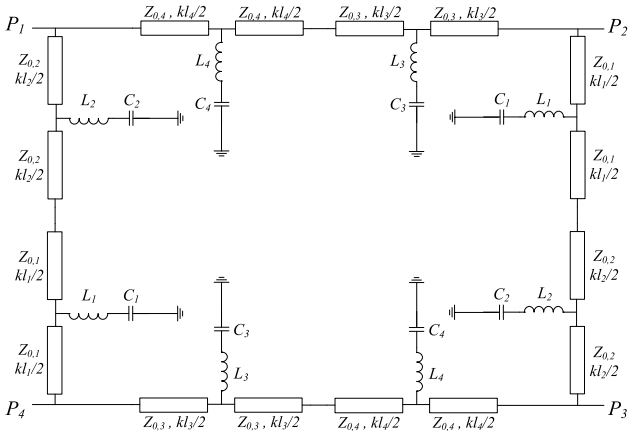

FIGURE 3. Schematic of the coupler based on slow-wave transmission lines.

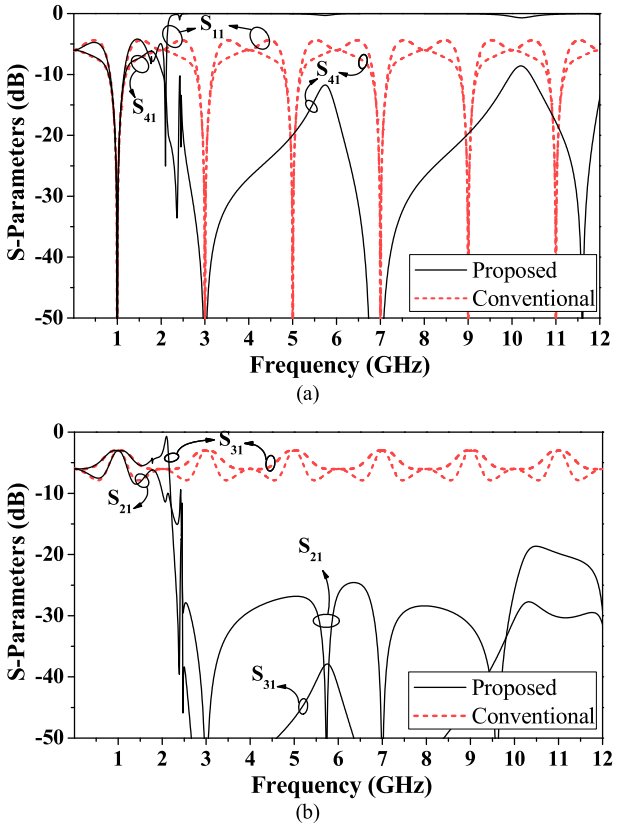

FIGURE 4. Response of the proposed coupler compared to the one of the conventional counterpart. (a) Matching (S_{11}) and isolation (S_{41}); (b) power splitting (S_{21} and S_{31}).

tion technology (an *LPKF H100* drilling machine), and we have adjusted the length to the convenient value in order to achieve the required value of the inductance. Nevertheless, for small inductance values, this may provide extremely short lengths, which are not convenient in order to avoid any potential coupling between the host line and the capacitor patches of the SISS resonators. For this reason, in some cases, the width of the inductive line is wider, providing longer

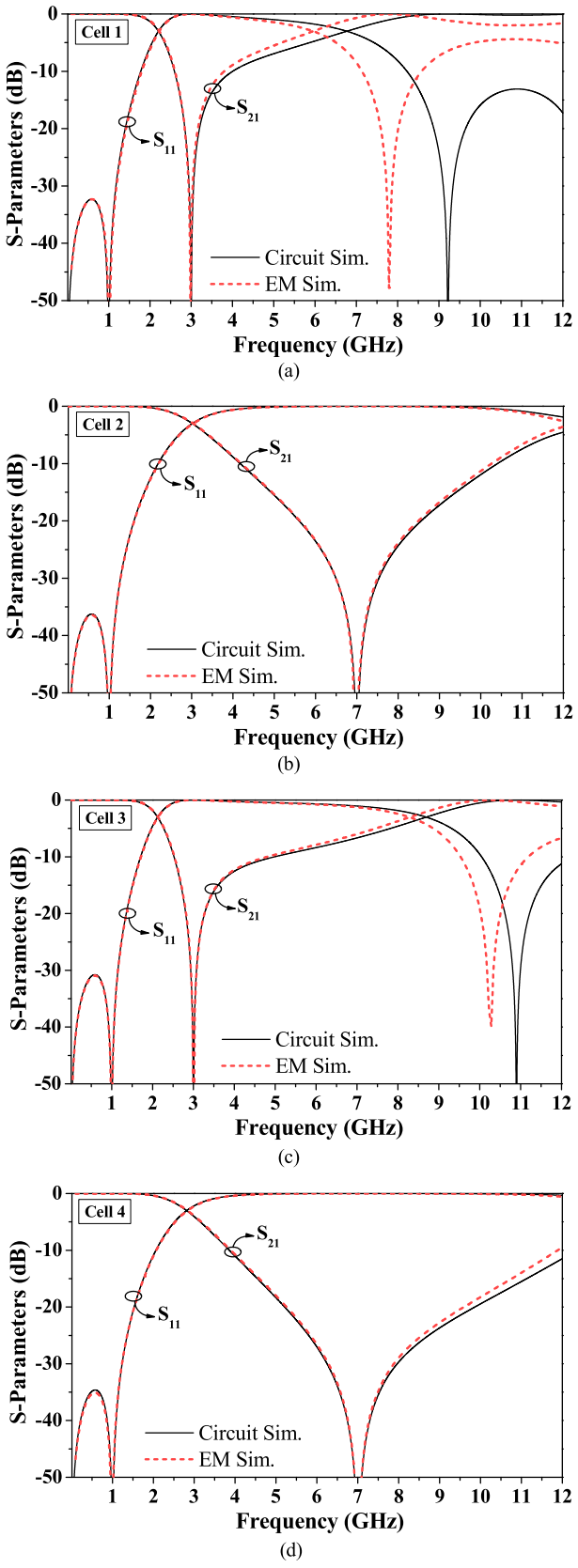

FIGURE 5. Circuit and lossless electromagnetic simulation of the responses of the four designed unit cells: (a) and (b) are the cells of the 50-Ω line pair; (c) and (d) correspond to the cells of the 35.35-Ω line pair.

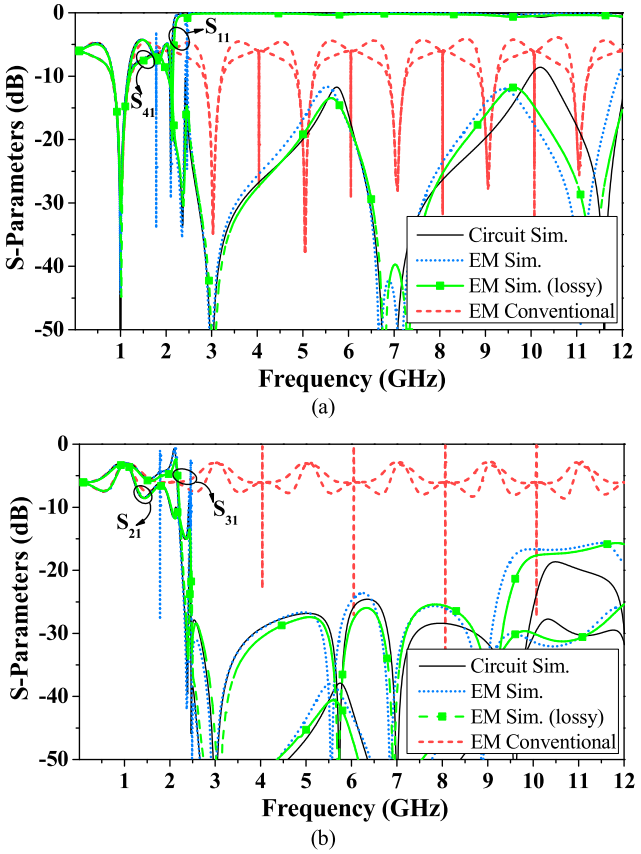

FIGURE 6. Circuit and electromagnetic simulation (with and without losses) of the designed branch line coupler. The response (lossless electromagnetic simulation) of the conventional coupler is also included in the figure. (a) Matching and isolation; (b) power splitting.

TABLE 2. Physical dimensions of each cell.

		Cell 1	Cell 2	Cell 3	Cell 4
Host line	W (mm)	0.18	0.18	0.25	0.25
	l (mm)	13.96	13.96	11.54	11.54
Capacitive patch	W_A (mm)	2.45	2.80	3.79	3.75
	l_A (mm)	2.20	2.70	3.04	3.50
Inductive line	W_B (mm)	0.20	0.50	0.20	0.88
	l_B (mm)	5.61	1.09	2.65	0.90

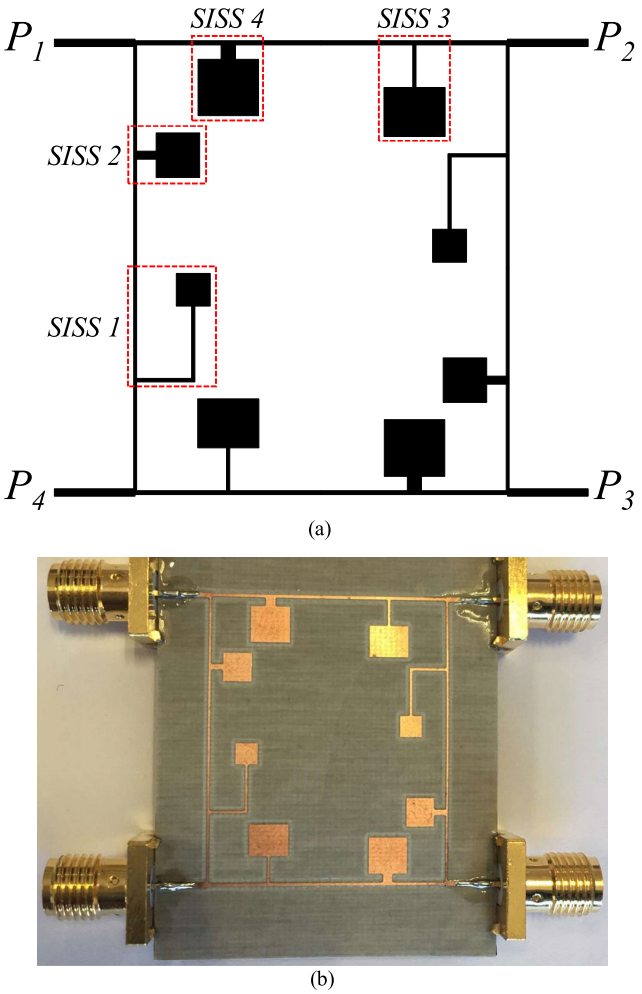

FIGURE 7. Layout (a) and photograph (b) of the designed and fabricated branch line coupler. The changed dimensions (in reference to Fig. 1 (b)) of the SISSs of the 50-Ω lines are $W_{A,1} = 2.10$ mm, $l_{A,1} = 2.03$ mm, $W_{B,1} = 0.20$ mm, $l_{B,1} = 8.11$ mm, $W_{A,2} = 2.77$ mm, $l_{A,2} = 2.70$ mm, $W_{B,2} = 0.5$ mm, $l_{B,2} = 1.30$ mm.

lines. The capacitor patches are indeed wide capacitive lines open-ended at the extreme. The width of these capacitive lines determines their length (according to the required capacitance value), and such width has been tuned in order to generate roughly square patches for the capacitances of the different SISSs. Previously to the generation of the layout of the whole branch line coupler, we have compared the lossless electromagnetic response of the four designed cells (including the host line and the SISS) with the circuit response. As mentioned, the electromagnetic simulations have been inferred by means of the *Momentum* simulator included in *Keysight ADS*, whereas the circuit simulations have been obtained by means of the schematic simulator of the same software tool (the details of the considered substrate have been given before). The results are depicted in Fig. 5, where an excellent match up to frequencies beyond the transmission zero frequency of the SISS can be appreciated. This indicates that the SISSs are correctly modeled by the corresponding series LC resonators up to frequencies substantially above the transmission zero. At higher frequencies, distributed effects are unavoidable, and for that reason discrepancies between the circuit and electromagnetic simulation arise. Such discrepancies are visible in Figs. 5a and 5c, corresponding to the cells with the transmission zero located at $3f_0$, but the agreement in Figs. 5b and 5d is excellent within the considered frequency range. Nevertheless, the discrepancies at high frequencies (for the indicated cells) are not relevant for the purpose of achieving efficient harmonic suppression, as it will be shown later.

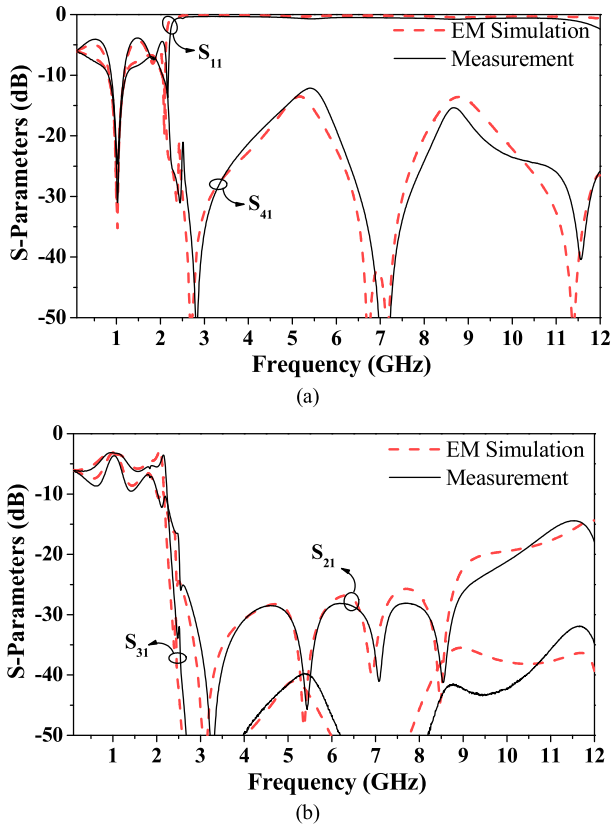

FIGURE 8. Measured and electromagnetic response (by including losses) of the designed and fabricated coupler. (a) Matching and isolation; (b) power splitting.

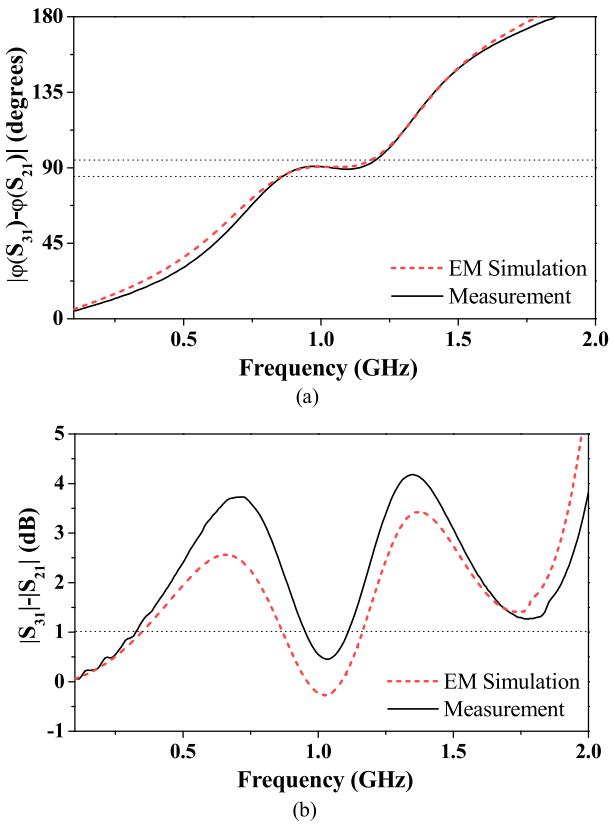

FIGURE 9. Phase (a) and amplitude (b) balance of the designed coupler. Small discrepancies are mainly attributed to fabrication related tolerances.

Then we have simulated the response of the whole branch line coupler, and the results are depicted in Fig. 6. Such figure includes the circuit response, as well as the electromagnetic response by excluding and including losses. The agreement between the circuit and the lossless electromagnetic simulation of the coupler is very good. The response that results by including substrate (dielectric) and metal (ohmic) losses does not differ so much of the lossless electromagnetic simulation. It can be seen that the response in the region of interest does not differ from the one of the conventional implementation. However, the harmonics are substantially rejected up to at least the 5-th harmonic, at $11f_0$.

It has been found that by fine tuning the position of the transmission zeros of two of the SISSs, the rejection efficiency of the harmonics, as well as the isolation, can be somehow improved. Note that any change in the transmission zero of the SISS does not modify the parameters of the host line of the corresponding cell, as far as the susceptance of the SISS, given by the solution of expressions (1)-(3), is not modified. The final layout of the coupler is the one depicted in Fig. 7, where the SISSs of the 50-Ω lines have been slightly modified (the transmission zeros have been set to 2.7 GHz and 6.8 GHz), and the corresponding dimensions are given in the caption of Fig. 7 (the other dimensions, given in Table 2, have not been altered).

The new response of the coupler (lossy electromagnetic simulation) is depicted in Fig. 8, where it can be appreciated that the isolation is better than 13.5 dB up to 12 GHz. We have fabricated the designed coupler (photograph depicted in Fig. 7), and we have measured the response by means of the *Keysight PNA N5221A* vector network analyzer. The agreement between the simulated and measured response is good (see Fig. 8). According to the measured response, the isolation level up to 12 GHz is better than 12.13 dB, in reasonable agreement to the predictions of the electromagnetic simulation. Concerning the filtering capability of the designed and fabricated coupler (useful for harmonic rejection), the measured rejection level for S_{21} is better than 16 dB up to $11f_0$, whereas for S_{31}, the suppression level is better than roughly 40 dB up to that frequency. This provides substantial rejection of the harmonics (see the comparative table in the next section). In the region of interest, the response of the designed coupler is good, with a power splitting of -3.17 dB and -3.69 dB, matching of -23.38 dB, and isolation of -26.55 dB at $f_0 = 1$ GHz.

It should be mentioned that due to the asymmetry of the SISS-loaded lines (with unequal SISS elements), the response of the coupler by considering port 2 as the input port is somehow different. However, such differences are very small (indeed negligible at the frequency of interest, f_0), and the same results concerning the suppression capability of the coupler prevail.

TABLE 3. Comparison with previously reported miniaturized branch line couplers.

Ref.	Relative Size (%)	Harmonic Suppression	Harmonic Suppression Level (dB) [a]	Miniaturization Method
[8]	48.7	No	-	Capacitive Loading
[11]	26.5	1st, 2nd	25/11	Capacitive Loading
[15]	26.8	No	-	Loaded Interdigital Capacitors
[23]	36	1st, 2nd	26/19	Artificial Lines with Capacitive-Inductive Loading
[28]	49.7	No	-	Slow-wave Structure Grounded Through Via-holes
[29]	46	1st, 2nd	25/32	Capacitive Loading
[30]	27	1st - 5th	40/27/40/45/28	Artificial Lines with Capacitive-Inductive Loading
[31]	15	1st, 2nd	20/35	Artificial Lines with High/Low TL Sections
[32]	15	1st, 2nd	20/35	Artificial Lines with High/Low TL Sections
[33]	12.4	No	-	Artificial Lines with High/Low TL Sections
[34]	36.5	1st	15	Meander T-shaped line
[35]	16.3 [b]	1st, 2nd	25/35	Artificial Lines with High/Low TL Sections
[36]	20.4	1st, 2nd	20/15	Capacitive Loading
[37]	9.4	No	-	Lumped capacitors and meander inductors
[42]	25	No	-	Loaded Open Stubs
[43]	45	No	-	T-Shaped Structure
[44]	24	1st	25	Compensated spiral compact microstrip resonant cell
[45]	29	No	-	T-Shaped Structure
[47]	58 [b]	1st, 2nd	25/25	Loaded Open Stubs
[48]	29.3	1st	30	Loaded Unequal Length Open Stubs
[49]	62.9 [b]	No	-	TLs Loaded with Lumped-distributed elements
[50]	40	No	-	Discontinuous Microstrip Lines
[51]	23.4 [b]	No	-	Loaded Open Stubs
[52]	13.9	No	-	Π-equivalent Artificial Lines
[53]	47	No	-	Dual Transmission Lines and Π-model
[54]	50	1st	30	Stepped Impedance TLs
[55]	66	No	-	Non-uniform Folded TL and SISS Loading
[56]	81.6	1st, 2nd	50/30	TLs Loaded with L-section (TL + open stub)
This work	**32.3**	**1st - 5th**	**35/30/37/26/16**	**Artificial Lines with Non-periodic SISS Loading**

[a] The worst rejection level from output ports has been chosen; [b] The best design has been considered

An important parameter in branch line hybrid couplers is the phase balance, or phase difference between the output ports. This parameter, as well as the amplitude balance, is depicted in Fig. 9. By considering a phase tolerance of $\pm 5°$, the resulting bandwidth for phase balance of the fabricated coupler has been found to be 0.34 GHz (or 34%). With regard to amplitude balance, the bandwidth has been found to be 0.159 GHz (or 15.9%), where, in this case, the maximum considered variation has been considered to be ± 1 dB.

IV. COMPARISON TO OTHER APPROACHES AND DISCUSSION

Table 3 includes information of various branch line couplers reported in the literature relative to size reduction and harmonic suppression capability (the main relevant aspects). It should be mentioned that the harmonic order in Table 3 refers to the intrinsic harmonic of the coupler. Note that branch line couplers exhibit their functionality at the odd harmonics only; therefore, the first (1st) harmonic refers to $3f_0$, the second (2nd) harmonic to $5f_0$, and so on. In view of the table, the coupler reported in [30] and the coupler reported in this work are those exhibiting better performance in terms of harmonic suppression bandwidth. In both cases, suppression up to at least the fifth harmonic band is demonstrated, whereas in the other couplers the suppressed harmonics do not extend beyond the second one (at $5f_0$). In [30], inductive and capacitive loading is used, and, according to the authors, series connected parallel resonant tanks generate transmission zeros useful for harmonic suppression. However, in [30], a detailed methodology for the design of the coupler is not reported. By contrast, in this paper, coupler design has been carried out according to clear guidelines, based on analytical expressions [23]. Moreover, the positions of the transmission zeros can be easily controlled, since the SISSs are very well described by series resonators, as it has been demonstrated in the previous section. Additionally, the agreement between the circuit schematic and the electromagnetic response of the layout of the coupler is very good, and this eases the design of the coupler as far as tuning the transmission zeros, a key aspect for harmonic suppression, can be done at the schematic level.

It should be mentioned, however, that, under some circumstances, it might be of interest to suppress the signals at $2f_0$, beyond the level that intrinsically branch line couplers do (e.g., due to the presence of nonlinear adjacent devices such as diodes or transistors). This aspect is discussed in [56], where the methodology for the design of branch line couplers with arbitrary power division ratios and harmonic

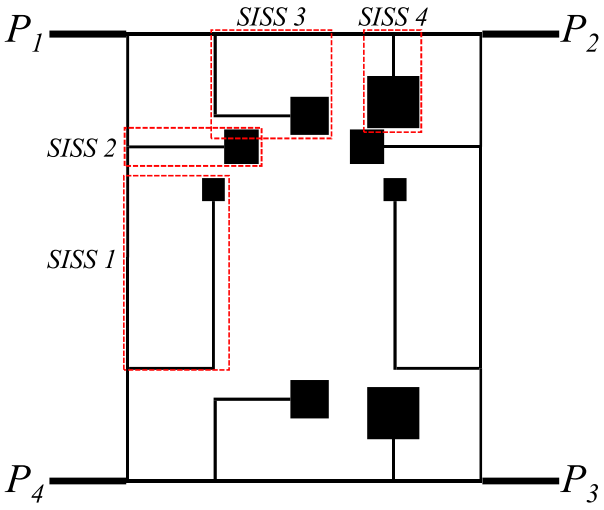

FIGURE 10. Layout of the second designed coupler.

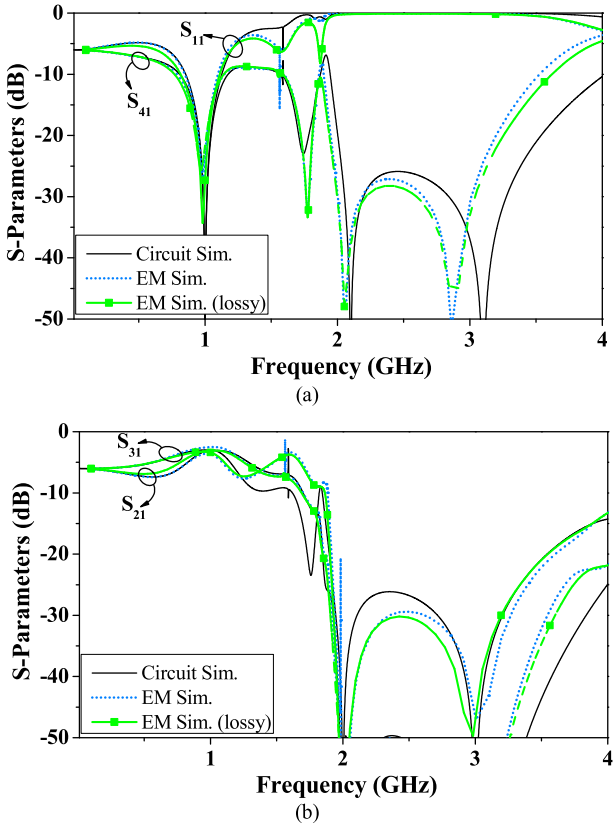

FIGURE 11. Circuit and electromagnetic simulation (with and without losses) of the second designed branch line coupler. (a) Matching and isolation; (b) power splitting.

TABLE 4. Electrical parameters for each transmission line section of the second designed coupler.

	Cell 1	Cell 2	Cell 3	Cell 4
Z_B (Ω)	50	50	35.35	35.35
βl (degrees)	45	45	45	45
swr	0.6	0.6	0.5	0.5
f_z/f_0	2.1	3.1	2	3
kl (degrees)	27	27	22.5	22.5
Z_0 (Ω)	86.27	86.27	73.61	73.61
L (nH)	4.970	1.968	3.447	1.293
C (pF)	1.156	1.339	1.837	2.177

suppression from $2f_0$ is pointed out. This recent work [56] achieves significant suppression of harmonics, by selectively locating transmission zeros at predefined positions by means of shunt stubs. The harmonic rejection level is better than roughly 30 dB between $2f_0$ (where a transmission zero is located) and $5f_0$ (corresponding to the 2nd intrinsic harmonic of the coupler, according to the above cited criterion). In this paper, our aim has been to reject the intrinsic harmonics of the coupler from $3f_0$, up the highest possible frequency ($11f_0$, in our case). Nevertheless, with our approach, it is also possible to reject potential signals present at $2f_0$. For that purpose, an option is to use a SISS element per transmission line section, which has the effect of driving the onset of the stop band to lower frequencies, as discussed in [14], [23]. The penalty is a slight degradation of the coupler bandwidth, as it is also visible in the couplers presented in [56], due to the presence of the transmission zero at $2f_0$.

Another option is to use the same topology already discussed in this work, but designing the SISS in order to achieve rejection at $2f_0$. To demonstrate this last possibility, we have made a new design of the coupler, by locating the transmission zeros of the SISSs at $2.1f_0$ and $3.1f_0$ in the 50-Ω line, and at $2f_0$ and $3f_0$ in the 35.35-Ω line. The design procedure is exactly the same as the one reported before. Table 4 shows the electrical parameters of the 50-Ω and 35.35-Ω SISS-loaded lines of the coupler, obtained by solving equations (1)-(5).

The layout of this second coupler, generated from the electrical parameters of either SISS-loaded line, is depicted in Fig. 10 (the substrate parameters are identical to those considered in the coupler of the previous section). The circuit and electromagnetic response of the designed coupler, with the first transmission zero at $2f_0$, is depicted in Fig. 11. It can be appreciated that the device is able to efficiently suppress any interfering signal present between $2f_0$ and $4f_0$. The rejection bandwidth is smaller than the one achieved in the previous coupler, but the new designed device is able to suppress any potential interfering signal present at $2f_0$. It should be noted, however, that the coupler in [56] is very efficient in suppressing the power splitting (S_{21} and S_{31}) between 2 GHz and 4GHz (both couplers operate at the same frequency).

We would like also to mention that our paper is devoted merely to the implementation of compact size and harmonic suppressed branch line hybrid couplers, with 3 dB power splitting, or equivalently, with the same power level

delivered to the output ports. If power division ratios different than 1 were required, high impedance transmission line sections are necessary. Since line loading with SISS resonators has the effect of increasing the impedance of the host line, the reported approach would jeopardize the physical implementation of the coupler. One possibility to solve this problem is to implement the lines with artificial lines based on inductive loading [18] or based on both capacitive and inductive loading [23]. In this case, the impedance of the host line is reduced (inductive loading), or it can be set to a convenient (implementable) value (simultaneous inductive and capacitive loading).

V. CONCLUSION

In conclusion, a branch line coupler with efficient harmonic suppression based on slow-wave artificial lines has been designed and fabricated. Such harmonic suppression, which extends up to at least $12f_0$ (f_0 being the design frequency), has been possible by loading the constitutive artificial lines of the coupler by means of a pair of step impedance shunt stubs (SISSs). Such SISSs behave as shunt connected series resonators, thereby providing a transmission zero at their resonance frequency. Thus, by designing the SISSs with different resonance frequencies (and with the required value of their susceptance), the generated transmission zeros, conveniently located, have been the key aspect to achieve a wide stop band above the region of interest. Moreover, since the SISSs exhibit a capacitive behavior in the region of interest (vicinity of f_0), the phase velocity of the lines has been reduced, and consequently the overall size of the coupler has been decreased as well. As compared to the conventional branch line coupler, the area occupied by the designed device is 67.7% smaller. The main contribution of the paper is the demonstration that, by truncating periodicity and by using series resonators (SISS) as loading reactive elements, branch line couplers with very efficient harmonic suppression, following a simple design methodology, can be implemented.

REFERENCES

[1] K. Wu, "Slow wave structures," in *Encyclopedia of Electrical and Electronics Engineering*, vol. 19, J. G. Webster, Ed. New York, NY, USA: Wiley, 1999, pp. 366–381.
[2] F. Martín, *Artificial Transmission Lines for RF and Microwave Applications*. Hoboken, NJ, USA: Wiley, 2015.
[3] T. Hirota, A. Minakawa, and M. Muraguchi, "Reduced-size branch-line and rat-race hybrids for uniplanar MMIC's," *IEEE Trans. Microw. Theory Techn.*, vol. 38, no. 3, pp. 270–275, Mar. 1990.
[4] A. Görür, "A novel coplanar slow-wave structure," *IEEE Microw. Guided Wave Lett.*, vol. 4, no. 3, pp. 86–88, Mar. 1994.
[5] A. Gorur, C. Karpuz, and M. Alkan, "Characteristics of periodically loaded CPW structures," *IEEE Microw. Guided Wave Lett.*, vol. 8, no. 8, pp. 278–280, Aug. 1998.
[6] R. B. Singh and T. M. Weller, "Miniaturized 20 GHz CPW quadrature coupler using capacitive loading," *Microw. Opt. Technol. Lett.*, vol. 30, no. 1, pp. 3–5, Jul. 2001.
[7] M. C. Scardelletti, G. E. Ponchak, and T. M. Weller, "Miniaturized wilkinson power dividers utilizing capacitive loading," *IEEE Microw. Wireless Compon. Lett.*, vol. 12, no. 1, pp. 6–8, Jan. 2002.
[8] K. W. Eccleston and S. H. M. Ong, "Compact planar microstripline branch-line and rat-race couplers," *IEEE Trans. Microw. Theory Techn.*, vol. 51, no. 10, pp. 2119–2125, Oct. 2003.
[9] J. García-García, J. Bonache, and F. Martín, "Application of electromagnetic bandgaps (EBGs) to the design of ultra wide band pass filters (UWBPFs) with good out-of-band performance," *IEEE Trans. Microw. Theory Techn.*, vol. 54, no. 12, pp. 4136–4140, Dec. 2006.
[10] C.-I. Shie, J.-C. Cheng, S.-C. Chou, and Y.-C. Chiang, "Transdirectional coupled-line couplers implemented by periodical shunt capacitors," *IEEE Trans. Microw. Theory Techn.*, vol. 57, no. 12, pp. 2981–2988, Dec. 2009.
[11] H. Cui, J. Wang, and J.-L. Li, "Compact microstrip branch-line coupler with wideband harmonic suppression," *ACES J.*, vol. 27, pp. 766–771, Sep. 2012.
[12] M. Orellana, J. Selga, M. Sans, A. Rodríguez, V. Boria, and F. Martín, "Synthesis of slow-wave structures based on capacitive-loaded lines through aggressive space mapping (ASM)," *Int. J. RF Microw. Comput.-Aided Eng.*, vol. 25, no. 7, pp. 629–638, Sep. 2015.
[13] J. Selga, P. Vélez, M. Orellana, A. Rodríguez, V. Boria, and F. Martín, "Size reduction and spurious suppression in microstrip coupled line bandpass filters by means of capacitive electromagnetic bandgaps," in *IEEE MTT-S Int. Microw. Symp. Dig.*, San Francisco, CA, USA, May 2016, pp. 22–27.
[14] M. Orellana, J. Selga, P. Vélez, A. Rodríguez, V. Boria, and F. Martín, "Design of capacitively-loaded coupled line bandpass filters with compact size and spurious suppression," *IEEE Trans. Microw. Theory. Techn.*, vol. 65, pp. 1235–1248, Jan. 2017.
[15] K.-Y. Tsai, H.-S. Yang, J.-H. Chen, and Y.-J.-E. Chen, "A miniaturized 3 dB branch-line hybrid coupler with harmonics suppression," *IEEE Microw. Wireless Compon. Lett.*, vol. 21, no. 10, pp. 537–539, Oct. 2011.
[16] L. Zhu, "Guided-wave characteristics of periodic microstrip lines with inductive loading: Slow-wave and bandstop behaviors," *Microw. Opt. Technol. Lett.*, vol. 41, no. 2, pp. 77–79, Apr. 2004.
[17] S. Lee and Y. Lee, "Generalized miniaturization method for coupled-line bandpass filters by reactive loading," *IEEE Trans. Microw. Theory Techn.*, vol. 58, no. 9, pp. 2383–2391, Sep. 2010.
[18] P. Vélez, J. Selga, J. Bonache, and F. Martín, "Slow-wave inductively-loaded electromagnetic bandgap (EBG) coplanar waveguide (CPW) transmission lines and application to compact power dividers," in *Proc. 46th Eur. Microw. Conf. (EuMC)*, London, U.K., Oct. 2016, pp. 3–7.
[19] J. Selga, P. Vélez, J. Bonache, and F. Martín, "EBG-based transmission lines with slow-wave characteristics and application to miniaturization of microwave components," *Appl. Phys. A, Solids Surf.*, vol. 123, no. 1, p. 44, Jan. 2017.
[20] S.-G. Mao and M.-Y. Chen, "A novel periodic electromagnetic bandgap structure for finite-width conductor-backed coplanar waveguides," *IEEE Microw. Wireless Compon. Lett.*, vol. 11, no. 6, pp. 261–263, Jun. 2001.
[21] J. Sor, Y. Qian, and T. Itoh, "Miniature low-loss CPW periodic structures for filter applications," *IEEE Trans. Microw. Theory Techn.*, vol. 49, no. 12, pp. 2336–2341, Dec. 2001.
[22] F. Aznar, J. Selga, A. Fernández-Prieto, J. Coromina, P. Vélez, J. Bonache, and F. Martín, "Slow wave coplanar waveguides based on inductive and capacitive loading and application to compact and harmonic suppressed power splitters," *Int. J. Microw. Wireless Technol.*, vol. 10, nos. 5–6, pp. 530–537, Jun. 2018, doi: 10.1017/S1759078717001350.
[23] J. Selga, P. Vélez, J. Coromina, A. Fernández-Prieto, J. Bonache, and F. Martín, "Harmonic suppression in branch-line couplers based on slow-wave transmission lines with simultaneous inductive and capacitive loading," *Microw. Opt. Techn. Lett.*, vol. 60, pp. 2374–2384, Oct. 2018.
[24] P. Vélez, F. Aznar-Ballesta, J. Coromina, J. Bonache, and F. Martín, "Compact coplanar waveguide power splitter with filtering capability based on slow-wave structures," *Microw. Opt. Technol. Lett.*, vol. 61, no. 5, pp. 1143–1148, May 2019.
[25] J. Selga, J. Coromina, P. Vélez, A. Fernández-Prieto, J. Bonache, and F. Martín, "Miniaturised and harmonic-suppressed rat-race couplers based on slow-wave transmission lines," *IET Microw., Antennas Propag.*, vol. 13, no. 9, pp. 1293–1299, Jul. 2019.
[26] H. Liu, S.-J. Fang, Z. Wang, and Y. Zhou, "Miniaturization of transdirectional coupled line couplers using series inductors," *Prog. Electromagn. Res. C*, vol. 46, pp. 171–177, Jan. 2014.
[27] A. Niembro-Martín, V. Nasserddine, E. Pistono, H. Issa, A. L. Franc, T.-P. Vuong, and P. Ferrari, "Slow-wave substrate integrated waveguide," *IEEE Trans. Microw. Theory Techn.*, vol. 62, pp. 1625–1633, Aug. 2014.
[28] Y. Morimoto, A. Waghmare, K. Dhwaj, and T. Itoh, "A compact branch line coupler using novel periodically grounded slow-wave structure," in *IEEE MTT-S Int. Microw. Symp. Dig.*, San Francisco, CA, USA, May 2016, pp. 22–27.

[29] J. Coromina, J. Selga, P. Vélez, J. Bonache, and F. Martín, "Size reduction and harmonic suppression in branch line couplers implemented by means of capacitively loaded slow-wave transmission lines," *Microw. Opt. Technol. Lett.*, vol. 59, no. 11, pp. 2822–2830, Nov. 2017.

[30] C.-W. Wang, T.-G. Ma, and C.-F. Yang, "Miniaturized branch-line coupler with harmonic suppression for RFID applications using artificial transmission lines," in *IEEE MTT-S Int. Microw. Symp. Dig.*, Honolulu, HI, USA, Jun. 2007, pp. 29–32.

[31] P. Kurgan, J. Filipcewicz, and M. Kitlinski, "Design considerations for compact microstrip resonant cells dedicated to efficient branch-line miniaturization," *Microw. Opt. Technol. Lett.*, vol. 54, no. 8, pp. 1949–1954, Aug. 2012.

[32] P. Kurgan, J. Filipcewicz, and M. Kitlinski, "Development of a compact microstrip resonant cell aimed at efficient microwave component size reduction," *IET Microw., Antennas Propag.*, vol. 6, no. 12, p. 1291, 2012.

[33] S. Koziel and P. Kurgan, "Low-cost optimization of compact branch-line couplers and its application to miniaturized butler matrix design," in *Proc. 44th Eur. Microw. Conf.*, Rome, Italy, Oct. 2014, pp. 227–230.

[34] K.-S. Choi, K.-C. Yoon, J.-Y. Lee, C.-K. Lee, S.-C. Kim, K.-B. Kim, and J.-C. Lee, "Compact branch-line coupler with harmonics suppression using meander T-shaped line," *Microw. Opt. Technol. Lett.*, vol. 56, no. 6, pp. 1382–1384, Jun. 2014.

[35] S. Koziel and P. Kurgan, "Rapid design of miniaturised branch-line couplers through concurrent cell optimisation and surrogate-assisted fine-tuning," *IET Microw., Antennas Propag.*, vol. 9, no. 9, pp. 957–963, Jun. 2015.

[36] G. Lian, Z. Wang, Z. He, Z. Zhong, L. Sun, and M. Yu, "A new miniaturized microstrip branch-line coupler with good harmonic suppression," *Prog. Electromagn. Res. Lett.*, vol. 67, pp. 61–66, Apr. 2017.

[37] H.-R. Ahn and S. Nam, "Compact microstrip 3-dB coupled-line ring and branch-line hybrids with new symmetric equivalent circuits," *IEEE Trans. Microw. Theory Techn.*, vol. 61, no. 3, pp. 1067–1078, Mar. 2013.

[38] J. Naqui, M. Durán-Sindreu, J. Bonache, and F. Martín, "Implementation of shunt-connected series resonators through stepped-impedance shunt stubs: Analysis and limitations," *IET Microw., Antennas Propag.*, vol. 5, pp. 1336–1342, Aug. 2011.

[39] J. Coromina, J. Selga, P. Velez, J. Bonache, and F. Martin, "Slow-wave artificial transmission lines based on stepped impedance shunt stub (SISS) loading: Analysis and stopband bandwidth enhancement," in *Proc. 48th Eur. Microw. Conf. (EuMC)*, Madrid, Spain, Sep. 2018, pp. 69–72.

[40] J. Coromina, P. Vélez, J. Bonache, F. Aznar-Ballesta, A. Fernández-Prieto, and F. Martín, "Reactively-loaded non-periodic slow-wave artificial transmission lines for stop band bandwidth enhancement: Application to power splitters," *Int. J. Microw. Wireless Technol.*, vol. 11, nos. 5–6, pp. 475–481, Jun. 2019.

[41] H.-R. Ahn and M. M. Tentzeris, "In-phase T-junction: Study and application to Gysel power dividers for high power-division ratios requiring no high-impedance transmission-line section," *IEEE Access*, vol. 7, pp. 18146–18154, Jul. 2019.

[42] M.-L. Chuang, "Miniaturized ring coupler of arbitrary reduced size," *IEEE Microw. Wireless Compon. Lett.*, vol. 15, no. 1, pp. 16–18, Jan. 2005.

[43] S.-S. Liao, P.-T. Sun, N.-C. Chin, and J.-T. Peng, "A novel compact-size branch-line coupler," *IEEE Microw. Wireless Compon. Lett.*, vol. 15, no. 9, pp. 588–590, Sep. 2005.

[44] J. Gu and X. Sun, "Miniaturization and harmonic suppression of branch-line and rat-race hybrid coupler using compensated spiral compact microstrip resonant cell," in *IEEE MTT-S Int. Microw. Symp. Dig.*, Los Angeles, CA, USA, Jun. 2005, pp. 1211–1214.

[45] S.-S. Liao and J.-T. Peng, "Compact planar microstrip branch-line couplers using the quasi-lumped elements approach with nonsymmetrical and symmetrical T-shaped structure," *IEEE Trans. Microw. Theory Techn.*, vol. 54, no. 9, pp. 3508–3514, Sep. 2006.

[46] J. Wang, B.-Z. Wang, Y.-X. Guo, L. C. Ong, and S. Xiao, "A compact slow-wave microstrip branch-line coupler with high performance," *IEEE Microw. Wireless Compon. Lett.*, vol. 17, no. 7, pp. 501–503, Jul. 2007.

[47] P. Mondal and A. Chakrabarty, "Design of miniaturised branch-line and rat-race hybrid couplers with harmonics suppression," *IET Microw., Antennas Propag.*, vol. 3, no. 1, pp. 109–116, Feb. 2009.

[48] V. K. Velidi, B. Patel, and S. Sanyal, "Harmonic suppressed compact wideband branch-line coupler using unequal length open-stub units," *Int. J. RF Microw. Comput.-Aided Eng.*, vol. 21, no. 1, pp. 115–119, Jan. 2011.

[49] Y.-H. Chun and J.-S. Hong, "Design of a compact broadband branch-line hybrid," in *IEEE MTT-S Int. Microw. Symp. Dig.*, Long Beach, CA, USA, Jun. 2005, pp. 997–1000.

[50] K.-O. Sun, S.-J. Ho, C.-C. Yen, and D. van der Weide, "A compact branch-line coupler using discontinuous microstrip lines," *IEEE Microw. Wireless Compon. Lett.*, vol. 15, no. 8, pp. 519–520, Aug. 2005.

[51] C.-W. Tang and M.-G. Chen, "Synthesizing microstrip branch-line couplers with predetermined compact size and bandwidth," *IEEE Trans. Microw. Theory Techn.*, vol. 55, no. 9, pp. 1926–1934, Sep. 2007.

[52] C.-H. Tseng and C.-H. Wu, "Design of compact branch-line couplers using π-equivalent artificial transmission lines," *IET Microw., Antennas Propag.*, vol. 6, no. 9, pp. 969–974, Jul. 2012.

[53] V. Iran-Nejad, A. A. Lotfi-Neyestanak, and A. Shahzadi, "Compact broadband quadrature hybrid coupler using planar artificial transmission line," *Electron. Lett.*, vol. 48, no. 25, pp. 1602–1603, Dec. 2012.

[54] S. H. Sedighy and M. K. Amirhosseini, "Compact branch line coupler using step impedance transmission lines (SITLs)," *Appl. Comput. Electromagn. Soc. J.*, vol. 28, no. 9, pp. 866–870, Sep. 2013.

[55] S. Nouri, J. Nourinia, N. Valizade, B. Mohammadi, and A. Valizade, "Novel compact branch-line coupler using non-uniform folded transmission line and shunt step impedance stub with harmonics suppressions," *Appl. Comput. Electromagn. Soc. J.*, vol. 31, no. 4, pp. 401–409, Apr. 2016.

[56] H.-R. Ahn and M. M. Tentzeris, "Arbitrary power-division branch-line hybrids for high-performance, wideband, and selective harmonic suppressions from $2f_0$," *IEEE Trans. Microw. Theory Techn.*, vol. 67, no. 3, pp. 978–987, Mar. 2019.

JAN COROMINA (Student Member, IEEE) was born in Barcelona, Spain, in 1989. He received the bachelor's degree in electronics engineering for telecommunication and the Telecommunication Engineering master's degree from the Universitat Autònoma de Barcelona (UAB), Barcelona, in 2014 and 2017, respectively, and the Ph.D. degree in microwave circuit design and miniaturization from CIMITEC, Departament d'Enginyeria Electrònica, UAB.

Specifically, his work is focused on the design of slow wave structures and their application to a diversity of microwave circuits. In 2016, he joined IDNEO Technologies as an RF engineer, where he developed ISM antennas for industrial applications and multiservice LNA for the automotive sector.

PARIS VÉLEZ (Member, IEEE) was born in Barcelona, Spain, in 1982. He received the degree in telecommunications engineering, specializing in electronics, the Electronics Engineering degree, and the Ph.D. degree in electrical engineering from the Universitat Autònoma de Barcelona, Barcelona, in 2008, 2010, and 2014, respectively. His Ph.D. thesis concerned common mode suppression differential microwave circuits based on metamaterial concepts and semi-lumped resonators. His current research interests include the miniaturization of passive circuits RF/microwave and sensors-based metamaterials through the Juan de la Cierva fellowship. During his Ph.D., he was awarded with the Pre-Doctoral Teaching and Research Fellowship by the Spanish Government, from 2011 to 2014. From 2015 to 2017, he was involved in the subjects related to metamaterials sensors for fluidics detection and characterization at LAAS-CNRS through the TECNIOSpring Fellowship, co-founded by the Marie Curie Program. He is currently a Reviewer of the IEEE TRANSACTIONS ON MICROWAVE THEORY AND TECHNIQUES and other journals.

JORDI BONACHE (Member, IEEE) was born in Cardona (Barcelona), Spain, in 1976. He received the Physics and Electronics Engineering degrees and the Ph.D. degree in electronics engineering from the Universitat Autònoma de Barcelona, in 1999, 2001, and 2007, respectively. In 2000, he joined the High Energy Physics Institute of Barcelona, where he was involved in the design and implementation of the control, and monitoring system of the MAGIC telescope. In 2001, he joined the Department of Electronics Engineering, Universitat Autònoma de Barcelona, where he is currently a Professor of electronics. From 2006 to 2009, he was an Executive Manager with CIMITEC, Spain, where he is currently the Project Manager and leads the research on RFID and antennas. His current research interests include active and passive microwave devices, metamaterials, antennas, and RFID.

FERRAN MARTíN (Fellow, IEEE) was born in Barakaldo (Vizcaya), Spain, in 1965. He received the B.S. degree in physics from the Universitat Autònoma de Barcelona (UAB), in 1988, and the Ph.D. degree, in 1992.

From 1994 to 2006, he was an Associate Professor of electronics with the Departament d'Enginyeria Electrònica, UAB, where he has been a Full Professor of electronics, since 2007. In recent years, he has been involved in different research activities, including modeling and simulation of electron devices for high-frequency applications, millimeter wave and THz generation systems, and the application of electromagnetic bandgaps to microwave and millimeter wave circuits. He is currently very active in the field of metamaterials and their application to the miniaturization and optimization of microwave circuits and antennas. Other topics of interest include microwave sensors and RFID systems, with special emphasis on the development of high-data capacity chipless-RFID tags. He is the Head of the Microwave Engineering, Metamaterials and Antennas Group (GEMMA Group), UAB, and the Director of CIMITEC, a Research Center on Metamaterials supported by TECNIO (Generalitat de Catalunya). He has authored or coauthored over 600 technical conference, letter, journal articles, and book chapters. He is the coauthor of the book on metamaterials entitled *Metamaterials With Negative Parameters: Theory, Design and Microwave Applications* (John Wiley and Sons Inc.) and *Time-Domain Signature Barcodes for Chipless-RFID and Sensing Applications* (Springer), the author of *Artificial Transmission Lines for RF and Microwave Applications* (John Wiley and Sons Inc.), and a Co-Editor of *Balanced Microwave Filters* (Wiley/IEEE Press). He has generated 19 Ph.D. students, has filed several patents on metamaterials, and has headed several development contracts. He is a Fellow of IET. He is also a member of the IEEE Microwave Theory and Techniques Society (IEEE MTT-S). He serves as a member of the Editorial Board for *IET Microwaves, Antennas & Propagation*, the *International Journal of RF and Microwave Computer-Aided Engineering*, and *Sensors*. He is also a member of the Technical Committees of the European Microwave Conference (EuMC) and the International Congress on Advanced Electromagnetic Materials in Microwaves and Optics (Metamaterials). Among his distinctions, he has received the 2006 Duran Farell Prize for Technological Research, he holds the Parc de Recerca UAB-Santander Technology Transfer Chair. He was a recipient of three ICREA ACADEMIA Awards (calls 2008, 2013, and 2018). He has organized several international events related to metamaterials and related topics, including Workshops at the IEEE International Microwave Symposium (in 2005 and 2007) and the European Microwave Conference (in 2009, 2015, and 2017) and the Fifth International Congress on Advanced Electromagnetic Materials in Microwaves and Optics (Metamaterials 2011), where he acted as the Chair of the Local Organizing Committee. He has acted as a Guest Editor of six special issues on *Metamaterials* and *Sensors* in five international journals. He is a Reviewer of the IEEE TRANSACTIONS ON MICROWAVE THEORY AND TECHNIQUES and the IEEE MICROWAVE AND WIRELESS COMPONENTS LETTERS, among many other journals.